Linearizing the soft finger contact constraint with application to dynamic force distribution in multifingered grasping

ZHENG Yu & QIAN Wenhan

Robotics Institute, Shanghai Jiao Tong University, Shanghai 200030, China
Correspondence should be addressed to Zheng Yu (email: yuzheng007@sjtu.edu.cn)

Received September 23, 2004

Abstract Currently, most efficient algorithms for force-closure analysis and dynamic force distribution utilize linear programming, but friction models are nonlinear. Substituting polyhedral cones for circular cones of Coulomb friction realizes the linearization of the frictional point contact constraint. So far, however, there is no approach to soft finger contact. This paper presents such an approach. Then the foregoing algorithms can be extended to grasping with soft finger contact. Herein an optimal force distribution algorithm for soft multifingered grasps is developed with an illustrative example.

Keywords: multifingered grasping, soft finger contact, linearization, force-closure, dynamic force distribution (DFD).

DOI: 10.1360/04ye0210

Multifingered grasping was ardently studied in the past two decades. Force-closure property and dynamic force distribution (DFD) are two basic topics. The former ensures that the contact forces of a grasp can equilibrate any external wrench. The latter seeks the optimal contact forces to equilibrate a dynamic external wrench. Force-closure is a prerequisite to stable grasps, while fast force distribution is required for real-time control of dexterous robot hands.

There are three common contact types: frictionless point contact, frictional point contact, and soft finger contact. Previous work[1—8] focused on the grasps with the former two. Only a few papers concern the last where the fingertip exerts a frictional spin moment about the inward contact normal besides a force. Howe et al.[9] suggested two friction models of soft finger contact. Buss et al.[10] transformed contact constraints into the positive definiteness of a certain linearly constrained matrix and proposed algorithms for force optimization[10,11]. Zuo and Qian[12] presented a force-closure test for soft-fingered grasps and put forward a DFD algorithm covering soft finger contact[13]. Han et al.[14] formulated the force-closure problem as a convex optimization problem involving linear matrix inequalities.

Linearizing circular cones of Coulomb friction at frictional point contacts by polyhedral convex cones, several efficient algorithms have been developed for force-closure test[2—4], force optimization[1,2], and grasp planning[6—8]. However, they cannot be applied to soft fingers, as linearization seems impossible when spin moments are involved. We attempt to fill this void. In fact, the soft finger contact constraint can be linearized as well, if we expand our idea from 3-D space to 4-D. Still the linearization can be viewed. Then the aforementioned algorithms[1—4,6—8] go generally applicable. A fast DFD algorithm for soft-fingered grasps is addressed first in this paper.

1 Preliminaries

Consider a soft m-fingered hand grasping an object, fixed with a right-handed coordinate frame. For soft finger contact, the contact force can be expressed in a local right-handed coordinate frame $\{\boldsymbol{n}_i, \boldsymbol{o}_i, \boldsymbol{t}_i\}$ by

$$\boldsymbol{f}_i = [\, f_{in} \quad f_{io} \quad f_{it} \quad f_{is} \,]^{\mathrm{T}}, \tag{1}$$

where f_{in} is the force component along the unit inward normal $\boldsymbol{n}_i$; f_{io} and f_{it} are the force components along the unit tangent vectors $\boldsymbol{o}_i$ and $\boldsymbol{t}_i$, respectively; f_{is} is the spin moment about $\boldsymbol{n}_i$; $\boldsymbol{n}_i$, $\boldsymbol{o}_i$, $\boldsymbol{t}_i$ are specified with respect to the object coordinate frame. The wrench exerted by the i-th fingertip can be computed by

$$\boldsymbol{w}_i = \boldsymbol{G}_i \boldsymbol{f}_i, \tag{2}$$

where

$$\boldsymbol{G}_i = \begin{bmatrix} \boldsymbol{n}_i & \boldsymbol{o}_i & \boldsymbol{t}_i & \boldsymbol{0} \\ \boldsymbol{r}_i \times \boldsymbol{n}_i & \boldsymbol{r}_i \times \boldsymbol{o}_i & \boldsymbol{r}_i \times \boldsymbol{t}_i & \boldsymbol{n}_i \end{bmatrix} \in \mathbb{R}^{6\times 4} \tag{3}$$

is the grasp matrix at contact i; $\boldsymbol{r}_i$ is the position vector in the object coordinate frame.

Let $\boldsymbol{w}$ and $\boldsymbol{w}_{\mathrm{ext}}$ denote the resultant wrench applied by the hand and the external wrench. For equilibrium

$$-\boldsymbol{w}_{\mathrm{ext}} = \boldsymbol{w} = \sum_{i=1}^{m} \boldsymbol{w}_i. \tag{4}$$

To avoid separation and slippage at contact, $\boldsymbol{f}_i$ must satisfy either condition[9—14] in (5) and (6) expressing its sets:

(i) Linear model

$$V_{li} = \left\{ \boldsymbol{f}_i \in \mathbb{R}^4 \,\middle|\, f_{in} \geqslant 0, \ \sqrt{\frac{f_{io}^2 + f_{it}^2}{m_i^2}} + \frac{|f_{is}|}{m_{si}} \leqslant f_{in} \right\}; \tag{5}$$

(ii) Elliptical model

$$V_{ei} = \left\{ \boldsymbol{f}_i \in \mathbb{R}^4 \middle| \, f_{in} \geqslant 0, \sqrt{\frac{f_{io}^2 + f_{it}^2}{\mu_i^2} + \frac{f_{is}^2}{\mu_{si}'^2}} \leqslant f_{in} \right\}, \tag{6}$$

where μ_i is Coulomb friction coefficient for the tangential force; μ_{si} and μ_{si}' are the coefficients of spin moment for the linear and elliptical models, respectively.

2 Linearization

The section hyperplanes of V_{li} and V_{ei} at $f_{in} = 1$ are

$$S_{li} = \left\{ t \in \mathbb{R}^3 \middle| \sqrt{\frac{t_1^2 + t_2^2}{\mu_i^2}} + \frac{|t_3|}{\mu_{si}} \leqslant 1 \right\}, \tag{7}$$

$$S_{ei} = \left\{ t \in \mathbb{R}^3 \middle| \sqrt{\frac{t_1^2 + t_2^2}{\mu_i^2} + \frac{t_3^2}{\mu_{si}'^2}} \leqslant 1 \right\}, \tag{8}$$

where t_1, t_2, t_3 are components of t. According to the above two models, S_{li} and S_{ei} represent the sets of allowable tangential force components and spin moments without slippage when the normal force component equals unity. S_{li} is a bicone of $\mathbb{R}^3$, while S_{ei} is an ellipsoid of $\mathbb{R}^3$, as shown in fig. 1. Comparing (5) with (7) and (6) with (8) we deduce: for soft finger contact, $\boldsymbol{f}_i \in V_{li}$ (resp. $\boldsymbol{f}_i \in V_{ei}$) if and only if $\boldsymbol{f}_i = r\,[1 \;\; \hat{\boldsymbol{o}}^{\mathrm{T}}]^{\mathrm{T}}$, where $r \geqslant 0$ and $t \in S_{li}$ (resp. $t \in S_{ei}$). This conclusion first clearly displays V_{li} and V_{ei}, though they are known to be convex cones[12]. It also implies that linearizing V_{li} and V_{ei} can be transformed to linearizing S_{li} and S_{ei}, respectively. This can be done by substituting a polyhedral bicone $\bar{S}_{li}$ and an oval polyhedron $\bar{S}_{ei}$ for S_{li} and S_{ei} (fig. 1). Formulated below, the vertices of $\bar{S}_{li}$ and $\bar{S}_{ei}$ fall on the boundaries of S_{li} and S_{ei}.

$$t_{ijk} = \left[\mu_i \cos\frac{2\pi j}{J}\cos\frac{\pi k}{2K} \quad \mu_i \sin\frac{j}{J}\cos\frac{k}{2K} \quad \mu_{si}\sin\frac{k}{2K} \right]^{\mathrm{T}}, \tag{9}$$

where $j = 1$ if $k = \pm K$, otherwise $j = 1, 2, \cdots, J$ $(J \geqslant 3)$; $k = -K, \cdots, -1, 0, 1, \cdots, K$ (K = 1 for $\bar{S}_{li}$; $K > 1$ and replace μ_{si} with μ_{si}' for $\bar{S}_{ei}$). Greater J and K improve the linearization quality but increase computation cost. For simplicity, we rearrange the vertices and shorten t_{ijk} to t_{ij}. Then the side edges for linearizing V_{li} and V_{ei} can be represented by

$$\boldsymbol{s}_{ij} = \left[1 \quad t_{ij}^{\mathrm{T}}\right]^{\mathrm{T}}, \quad j = 1, 2, \cdots, l \quad (l = 2JK - J + 2). \tag{10}$$

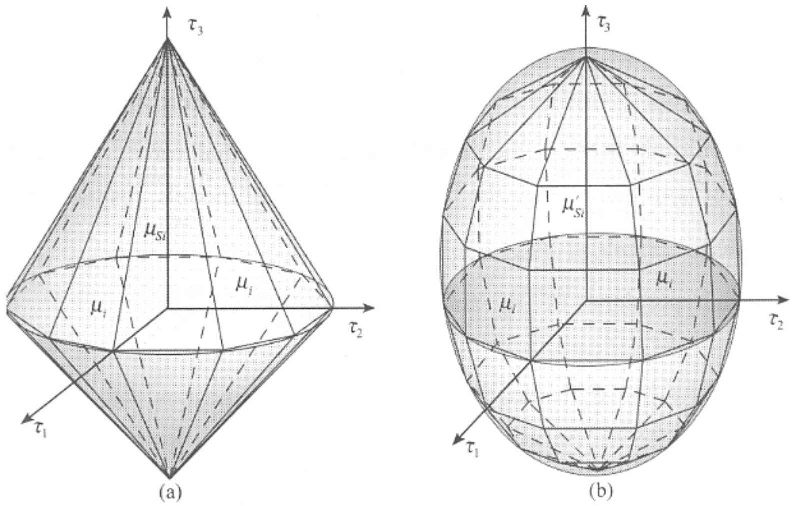

Fig. 1. Linearization of the linear model (a) and the elliptical model (b).

The contact force at the *i*-th soft finger contact is given by

$$\boldsymbol{f}_i = \sum_{j=1}^{l} l_{ij}\boldsymbol{s}_{ij}, \quad l_{ij} \geqslant 0 \quad \text{for} \quad j = 1, 2, \cdots, l. \tag{11}$$

Combining (1), (10) and (11) leads to

$$f_{in} = \sum_{j=1}^{l} l_{ij}. \tag{12}$$

Substituting (11) into (2) yields

$$\boldsymbol{w}_i = \sum_{j=1}^{l} l_{ij}\boldsymbol{w}_{ij}, \tag{13}$$

where

$$\boldsymbol{w}_{ij} = \boldsymbol{G}_i\boldsymbol{s}_{ij}. \tag{14}$$

Vectors $\boldsymbol{w}_{ij}$ are called *primitive wrenches*. From (4) and (13) we end up with

$$-\boldsymbol{w}_{\text{ext}} = \boldsymbol{w} = \sum_{i=1}^{m}\sum_{j=1}^{l} l_{ij}\boldsymbol{w}_{ij} = \boldsymbol{W}\,l, \tag{15}$$

where $\boldsymbol{W} = [\boldsymbol{w}_{11} \cdots \boldsymbol{w}_{ij} \cdots \boldsymbol{w}_{ml}] \in \mathbb{R}^{6\times ml}$ and $l = [l_{11} \cdots l_{ij} \cdots l_{ml}]^{\mathrm{T}} \in \mathbb{R}^{ml}$.

Being a 6-D polytope, the convex hull of the primitive wrenches $\boldsymbol{w}_{ij}$ is thereby

$$Q=\left\{\boldsymbol{w}=\sum_{i=1}^{m}\sum_{j=1}^{l}a_{ij}\boldsymbol{w}_{ij}\ \middle|\ \sum_{i=1}^{m}\sum_{j=1}^{l}a_{ij}=1,\ a_{ij}\geqslant 0 \text{ for } i=1,2,\cdots,m,\ j=1,2,\cdots,l\right\}. \tag{16}$$

We reason furthermore: (i) an external wrench $\boldsymbol{w}_{\text{ext}}$ can be equilibrated if and only if $-\boldsymbol{w}_{\text{ext}}$ can be expressed by a nonnegative combination of the primitive wrenches $\boldsymbol{w}_{ij}$; (ii) a grasp is force-closure if and only if the origin of the wrench space is an interior point of Q. Although acknowledged already[2—4,6—8], the above principles were limited to frictionless and frictional point contacts. Now we get rid of this limitation and the primitive wrenches here include those from the frictional spin moments.

3 Application to DFD

3.1 Problem statement

Given: A force-closure grasp (so $\boldsymbol{W}$ is settled) and a dynamic external wrench $\boldsymbol{w}_{\text{ext}}$.

Find: The optimal contact forces at the fingertips, such that s (summation of normal force components at all the contacts) becomes minimum.

Following Han et al.[14], we adopt s as the objective function (but our approach hereafter is brand-new), because generally a smaller s means smaller contact forces and smaller actuator power.

From (12) we obtain

$$s=\sum_{i=1}^{m}f_{in}=\sum_{i=1}^{m}\sum_{j=1}^{l}l_{ij}=\|\boldsymbol{l}\|_1, \tag{17}$$

where $\|\bullet\|_1$ denotes 1-norm.

Eq. (17) shows that the summation s of all the normal force components just equals the 1-norm of the coefficient vector $\boldsymbol{l}$. Thus the problem is to find $\boldsymbol{l}$ of the least 1-norm satisfying (15). In addition, from (16) and (17) Q is the set of all resultant wrenches exerted by the grasp when the summation of all the normal force components is unity.

3.2 A linearization based solution

Eq. (15) can be rewritten as

$$-\boldsymbol{w}_{\text{ext}}=s\sum_{i=1}^{m}\sum_{j=1}^{l}\frac{l_{ij}}{s}\boldsymbol{w}_{ij}=s\,\boldsymbol{x}, \tag{18}$$

where the second equal sign gives the definition of $\boldsymbol{x}$.

Equality (18) indicates that the point $\boldsymbol{x}$ is on the half-line $-\boldsymbol{w}_{\text{ext}}$ (from the origin of the wrench space to the point $-\boldsymbol{w}_{\text{ext}}$) and

$$s = \frac{\|\boldsymbol{w}_{\text{ext}}\|_1}{\|\boldsymbol{x}\|_1}. \tag{19}$$

From (16), (17) and (18) we see that $\boldsymbol{x} \in Q$. Thus $\boldsymbol{x}$ is a resultant wrench along $-\boldsymbol{w}_{\text{ext}}$ exerted by the grasp subject to the summation of all the normal force components being unity. From (19), s attains a minimum when $\boldsymbol{x}$ is the intersection point $\boldsymbol{x}_e$ of the half-line $-\boldsymbol{w}_{\text{ext}}$ with the boundary ∂Q of Q, since $\|\boldsymbol{x}\|_1$ therein is maximum. Furthermore, $\boldsymbol{x}_e$ can be expressed by a convex combination of only the primitive wrenches $\boldsymbol{w}_{ij}$ that fall on a hyperplane supporting Q at $\boldsymbol{x}_e$. According to (18), $-\boldsymbol{w}_{\text{ext}}$ can be restricted to a nonnegative combination of only such primitive wrenches. Let us partition $\boldsymbol{W}$ into $\boldsymbol{W}_1$ and $\boldsymbol{W}_2$, where $\boldsymbol{W}_1$ comprises such primitive wrenches and $\boldsymbol{W}_2$ consists of the others. Correspondingly, the coefficient vector l is partitioned into l_1 and l_2. Due to (15), we have

$$l_1 = -\boldsymbol{W}_1^{+}\boldsymbol{w}_{\text{ext}}, \quad l_2 = 0, \tag{20}$$

where $\boldsymbol{W}_1^{+}$ is the pseudoinverse of $\boldsymbol{W}_1$. The components of l_1 from (20) are all nonnegative because $-\boldsymbol{w}_{\text{ext}}$ is inside the convex cone decided by the columns of $\boldsymbol{W}_1$ and the origin.

In what follows, we seek a hyperplane supporting Q at $\boldsymbol{x}_e$, which is the key to the solution. For this, we first derive a new theorem in convex analysis, starting with two definitions[15]. Let Q^* be the polar set of Q, which is defined by

$$Q^* = \left\{\boldsymbol{u} \in \mathbb{R}^6 \,\middle|\, \boldsymbol{w}^{\mathrm{T}}\boldsymbol{u} \leqslant 1 \text{ for all } \boldsymbol{w} \in Q\right\}. \tag{21}$$

Recalling (16), rewrite (21) as

$$Q^* = \left\{\boldsymbol{u} \in \mathbb{R}^6 \,\middle|\, \boldsymbol{w}_{ij}^{\mathrm{T}}\boldsymbol{u} \leqslant 1 \text{ for } i = 1, 2, \cdots, m,\ j = 1, 2, \cdots, l\right\}, \tag{22}$$

which is also a 6-D polytope.

Let p be the support function of Q^*, which is the real-valued function defined by

$$p(\boldsymbol{z}) = \sup_{\boldsymbol{u} \in Q^*} \boldsymbol{z}^{\mathrm{T}}\boldsymbol{u}, \tag{23}$$

where $\boldsymbol{z}$ is a point other than the origin.

It follows directly from (23) that:

(I) $\boldsymbol{z}^{\mathrm{T}}\boldsymbol{u} \leqslant p(\boldsymbol{z})$ for all $\boldsymbol{u} \in Q^*$.

(II) There exists a point $\boldsymbol{u}_b \in \partial Q^*$ such that $p(\boldsymbol{z}) = \boldsymbol{z}^{\mathrm{T}}\boldsymbol{u}_b$.

(III) $p(\boldsymbol{z})>0$ if Q^* contains the origin as an interior point. Since the grasp is force-closure, both Q and Q^* satisfy this condition.

Additionally, convex analysis[15] tells us:

(IV) $Q^{**}=Q$, where $Q^{**}=(Q^*)^*$.

Theorem 1. The following statements are true:

(i) $p(\boldsymbol{z})^{-1}\boldsymbol{z}\in\partial Q$.

(ii) The hyperplane $H=\left\{\boldsymbol{w}\in\mathbb{R}^6 \,\middle|\, \boldsymbol{u}_b^{\mathrm{T}}\boldsymbol{w}=1\right\}$ supports Q at the point $p(\boldsymbol{z})^{-1}\boldsymbol{z}$.

Proof. (i) From (I) and (III), $p(\boldsymbol{z})^{-1}\boldsymbol{z}^{\mathrm{T}}\boldsymbol{u}\leqslant 1$ for all $\boldsymbol{u}\in Q^*$, which means $p(\boldsymbol{z})^{-1}\boldsymbol{z}\in Q^{**}$. Then from (IV), we have $p(\boldsymbol{z})^{-1}\boldsymbol{z}\in Q$. Suppose that there is a closed ball $B(r,p(\boldsymbol{z})^{-1}\boldsymbol{z})$ of radius $r>0$ centered at $p(\boldsymbol{z})^{-1}\boldsymbol{z}$. Let $\boldsymbol{y}=p(\boldsymbol{z})^{-1}\boldsymbol{z}+r\boldsymbol{z}/\|\boldsymbol{z}\|$. Obviously, $\boldsymbol{y}\in B(r,p(\boldsymbol{z})^{-1}\boldsymbol{z})$. But from (II) and (III), $\boldsymbol{y}^{\mathrm{T}}\boldsymbol{u}_b=p(\boldsymbol{z})^{-1}\boldsymbol{z}^{\mathrm{T}}\boldsymbol{u}_b+r\boldsymbol{z}^{\mathrm{T}}\boldsymbol{u}_b/\|\boldsymbol{z}\|=1+rp(\boldsymbol{z})/\|\boldsymbol{z}\|>1$, which means $\boldsymbol{y}\notin Q^{**}$ and $\boldsymbol{y}\notin Q$. Therefore $p(\boldsymbol{z})^{-1}\boldsymbol{z}\in\partial Q$.

(ii) From (II) it follows that $\boldsymbol{u}_b^{\mathrm{T}}p(\boldsymbol{z})^{-1}\boldsymbol{z}=1$, and thus $p(\boldsymbol{z})^{-1}\boldsymbol{z}\in H$. In addition, from (21) $\boldsymbol{u}_b^{\mathrm{T}}\boldsymbol{w}\leqslant 1$ for all $\boldsymbol{w}\in Q$, which means that H bounds Q. Q.E.D.

By substituting $-\boldsymbol{w}_{\mathrm{ext}}$ for all $\boldsymbol{z}$ above, Theorem 1(i) indicates $\boldsymbol{x}_e=-p(-\boldsymbol{w}_{\mathrm{ext}})^{-1}\boldsymbol{w}_{\mathrm{ext}}$. Substituting it into (19) yields the minimum value $s_{\min}=p(-\boldsymbol{w}_{\mathrm{ext}})$. Actually, the goal of the problem is neither $\boldsymbol{x}_e$ nor $s_{\min}$, but a hyperplane supporting Q at $\boldsymbol{x}_e$. Theorem 1(ii) indicates that H is just the hyperplane we are looking for, where $\boldsymbol{u}_b$ and $p(-\boldsymbol{w}_{\mathrm{ext}})$ can be found by (II) and (23).

3.3 Algorithm procedure

The algorithm can be summarized as:

Step 1. Linearize friction models by (10) and calculate primitive wrenches by (14).

Step 2. Compute $\boldsymbol{u}_b$. From (22) and (23), $\boldsymbol{u}_b$ is the optimal solution of the following linear programming problem:

$$\begin{cases}\text{Maximize } -\boldsymbol{w}_{\mathrm{ext}}^{\mathrm{T}}\boldsymbol{u},\\ \text{subject to } \boldsymbol{w}_{ij}^{\mathrm{T}}\boldsymbol{u}\leqslant 1,\ i=1,2,\cdots,m,\ j=1,2,\cdots,l.\end{cases} \tag{24}$$

Step 3. Partition $\boldsymbol{W}$ into $\boldsymbol{W}_1$ and $\boldsymbol{W}_2$ by testing $\boldsymbol{w}_{ij}$ one by one. If $\boldsymbol{u}_b^{\mathrm{T}}\boldsymbol{w}_{ij} = 1$, then this $\boldsymbol{w}_{ij}$ falls on H and joins $\boldsymbol{W}_1$, otherwise it joins $\boldsymbol{W}_2$.

Step 4. Compute l by (20).

Step 5. Compute $\boldsymbol{f}_i$, $i = 1, 2, \cdots, m$ by (11).

3.4 Computation cost

The first step calculates ml primitive wrenches. The problem (24) in Step 2 can be solved in $O(ml)$ time. Step 3 takes $O(ml)$ time to find the primitive wrenches $\boldsymbol{w}_{ij}$ on the hyperplane H, which are commonly much less than ml. Thus computing $\boldsymbol{W}_1^{+}$ does not need much computation cost. In Step 4, l is computed by (20) in only $O(1)$ time. Step 5 also takes $O(ml)$ time. To sum up, the time complexity of the algorithm is $O(ml)$ and *linear* with the finger number, essentially faster than the *polynomial* time complexity of Han et al.'s algorithm[14].

4 Numerical example

Fig. 2 depicts a soft three-fingered hand manipulating a conical flask of mass M = 0.1 kg. Its motion consists of the whirling about the axis $\boldsymbol{z}_0$ of the spatial coordinate frame $\{\boldsymbol{x}_0, \boldsymbol{y}_0, \boldsymbol{z}_0\}$ and the rotation about the axis $\boldsymbol{z}_b$ of the object coordinate frame $\{\boldsymbol{x}_b, \boldsymbol{y}_b, \boldsymbol{z}_b\}$ with its origin at the mass center. The two axes intersect at O with angle $j = p/12$, and the distance between O and the mass center is a = 0.12 m. The origin of the frame $\{\boldsymbol{x}_0, \boldsymbol{y}_0, \boldsymbol{z}_0\}$ is located at the projection of the mass center onto $\boldsymbol{z}_0$. The motion can be described by g_{0b}[16], the trajectory of the frame $\{\boldsymbol{x}_b, \boldsymbol{y}_b, \boldsymbol{z}_b\}$ relative to the frame $\{\boldsymbol{x}_0, \boldsymbol{y}_0, \boldsymbol{z}_0\}$,

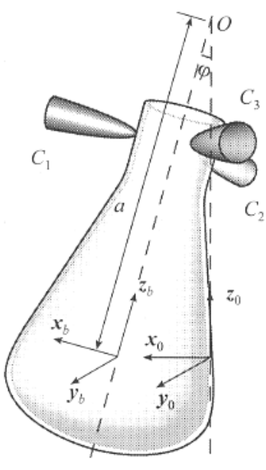

Fig. 2. A whirling flask.

$$g_{0b} = \begin{bmatrix} e^{\hat{w}_2 \hat{q}_2} & (I - e^{\hat{w}_2 q_2})\boldsymbol{q} \\ 0 & 1 \end{bmatrix} \begin{bmatrix} e^{\hat{w}_1 q_1} & 0 \\ 0 & 1 \end{bmatrix} \begin{bmatrix} e^{\hat{w}_0 j} & 0 \\ 0 & 1 \end{bmatrix} \equiv \begin{bmatrix} R_{0b} & \boldsymbol{p}_{0b} \\ 0 & 1 \end{bmatrix},$$

where q_1 and q_2 are the rotation angles about $\boldsymbol{z}_0$ and $\boldsymbol{z}_b$, respectively; $w_0 = [0 \quad 1 \quad 0]^{\mathrm{T}}$ gives the initial configuration, $w_1 = [0 \quad 0 \quad 1]^{\mathrm{T}}$ and $w_2 = [\sin j \cos q_1 \quad \sin j \sin q_1 \quad -\cos j]^{\mathrm{T}}$ denote the rotational axes, and $\hat{w}_0, \hat{w}_1, \hat{w}_2$ are the cross-product matrices for them; $\boldsymbol{I}$ is the identity matrix; $\boldsymbol{q} = [0 \quad 0 \quad a\cos j]^{\mathrm{T}}$. Set

$\dot{q}_1 = 2p$ rad/s, $\dot{q}_2 = 2p/3$ rad/s, $\ddot{q}_1 = \ddot{q}_2 = 0$ rad/s^2. The required resultant wrench can be computed by the well-known *Newton-Euler* equation:

$$\boldsymbol{w} = \begin{bmatrix} M\boldsymbol{I} & 0 \\ 0 & \boldsymbol{T} \end{bmatrix} \begin{bmatrix} \dot{\boldsymbol{v}}^b \\ \dot{\boldsymbol{\omega}}^b \end{bmatrix} + \begin{bmatrix} \boldsymbol{\omega}^b \times M\boldsymbol{v}^b \\ \boldsymbol{\omega}^b \times \boldsymbol{T}\boldsymbol{\omega}^b \end{bmatrix} + \begin{bmatrix} \boldsymbol{R}_{0b}^T \boldsymbol{g} \\ 0 \end{bmatrix},$$

where $\boldsymbol{T}$ is the inertia tensor, $\boldsymbol{v}^b = \boldsymbol{R}_{0b}^T \dot{\boldsymbol{p}}_{0b}$, $w^b = (\boldsymbol{R}_{0b}^T \dot{\boldsymbol{R}}_{0b})^{\vee}$, $\boldsymbol{g} = [0 \quad 0 \quad 9.8]^{\mathrm{T}}$ m/s^2.

The contact positions are: $\boldsymbol{r}_1 = [16 \quad 0 \quad 105]^{\mathrm{T}}$, $\boldsymbol{r}_2 = \left[-8 \quad -8\sqrt{3} \quad 105\right]^{\mathrm{T}}$, $\boldsymbol{r}_3 = \left[-8 \quad 8\sqrt{3} \quad 105\right]^{\mathrm{T}}$ (unit: mm). The coefficients of Coulomb friction and spin moment m = 0.2, m_s = 0.4 mm.

We implement the proposed algorithm using Matlab. Employ (3) to reckon the grasp matrix at each contact:

$$\boldsymbol{G}_1 = \begin{bmatrix} -1 & 0 & 0 & 0 \\ 0 & 0 & 1 & 0 \\ 0 & 1 & 0 & 0 \\ 0 & 0 & -105 & -1 \\ -105 & -16 & 0 & 0 \\ 0 & 0 & 16 & 0 \end{bmatrix}, \quad \boldsymbol{G}_2 = \begin{bmatrix} 0.50 & 0 & 0.87 & 0 \\ 0.87 & 0 & -0.50 & 0 \\ 0 & 1.0 & 0 & 0 \\ -90.93 & -13.86 & 52.50 & 0.50 \\ 52.50 & 8.0 & 90.93 & 0.87 \\ 0 & 0 & 16.0 & 0 \end{bmatrix},$$

$$\boldsymbol{G}_3 = \begin{bmatrix} 0.50 & 0 & -0.87 & 0 \\ -0.87 & 0 & -0.50 & 0 \\ 0 & 1.0 & 0 & 0 \\ 90.93 & 13.86 & 52.50 & 0.50 \\ 52.50 & 8.0 & -90.93 & -0.87 \\ 0 & 0 & 16.0 & 0 \end{bmatrix}.$$

Taking $J = 10$ and $K = 1$ in (10), we get 36 primitive wrenches from (14). Fig. 3 shows the contact forces produced by the DFD algorithm. The required CPU time on Pentium-IV PC for a point is 26.6 ms.

5 Conclusion

The linear and elliptical friction models of soft finger contact constraint can be regarded as two 4-D convex cones. We linearize them by linearizing their section hyperplanes, which are 3-D and visible (fig. 1). Then two basic principles concerning force-closure are generalized to all types of contact. Aided by a new theorem in convex analysis, a general and fast DFD algorithm comes out. By modifying certain equations properly, the theory and the methods in this paper can be applied to mixed use of the three contact types without difficulty.

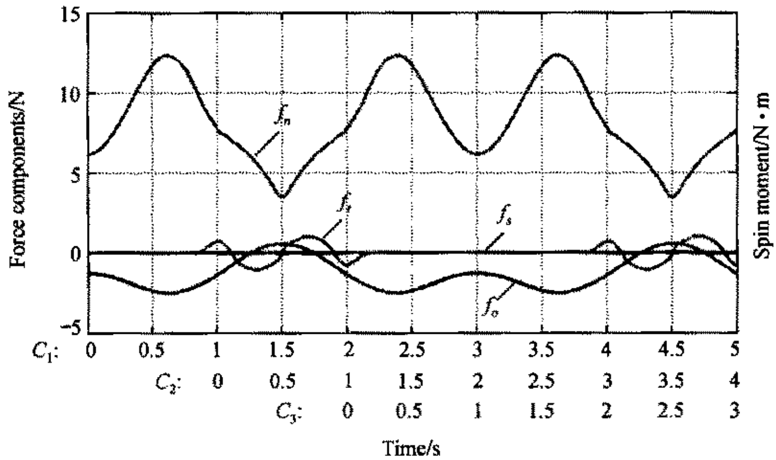

Fig. 3. The contact forces at fingertips.

References

1. Cheng, F. T., Orin, D. E., Efficient algorithm for optimal force distribution—The compact-dual LP method, IEEE Trans. Robot. Automat., 1990, 6(2): 178—187.
2. Liu, Y. H., Qualitative test and force optimization of 3-D frictional form-closure grasps using linear programming, IEEE Trans. Robot. Automat., 1999, 15(1): 163—173.
3. Mishra, B., Schwarz, J. T., Sharir, M., On the existence and synthesis of multifingered positive grips, Algorithmica, 1987, 2(4): 541—558.
4. Chen, I. M., Burdick, J. W., A qualitative test for N-finger force closure grasps on planar objects with applications to manipulation and finger gaits, in Proc. of IEEE Int. Conf. Robotics and Automation, Atlanta, Los Alamitos: IEEE Computer Society Press, 1993, 814—820.
5. Bicchi, A., On the closure properties of robotic grasping, Int. J. Robot. Res., 1995, 14(4): 319—334.
6. Ferrari, C., Canny, J., Planning optimal grasps, in Proc. of IEEE Int. Conf. Robotics and Automation, San Francisco, Washington, D. C.: IEEE Computer Society Press, 1992, 2290—2295.
7. Ding, D., Liu, Y. H., Wang, S. G., Computation of 3-D form-closure grasps, IEEE Trans. Robot. Automat., 2001, 17(4): 515—522.
8. Zhu, X. Y., Wang, J., Synthesis of force-closure grasps on 3-D objects based on the Q distance, IEEE Trans. Robot. Automat., 2003, 19(4): 669—679.
9. Howe, R. D., Kao, I., Cutkosky, M. R., The sliding of robot fingers under combined torsion and shear loading, Proc. IEEE Int. Conf. Robotics and Automation, Philadelphia, Washington, D. C.: IEEE Computer Society Press, 1988, 103—105.
10. Buss, M., Hashimoto, H., Moore, J. B., Dextrous hand grasping force optimization, IEEE Trans. Robot. Automat., 1996, 12(3): 406—417.
11. Buss, M., Faybusovich, L., Moore, J. B., Dikin-type algorithms for dextrous grasping force optimization, Int. J. Robot. Res., 1998, 17(8): 831—839.
12. Zuo, B. R., Qian, W. H., A force-closure test for soft multi-fingered grasps, Science in China, Ser. E, 1998, 41(1): 62—67.
13. Zuo, B. R., Qian, W. H., A general dynamic force distribution algorithm for multifingered grasping, IEEE Trans. Syst. Man Cybern. B, 2000, 30(1): 185—192.
14. Han, L., Trinkle, J. C., Li, Z. X., Grasp analysis as linear matrix inequality problems, IEEE Trans. Robot. Automat., 2000, 16(6): 663—674.
15. Lay, S. R., Convex Sets and Their Applications, New York: John Wiley & Sons, 1982, 140—143, 205—207.
16. Murray, R. M., Li, Z. X., Sastry, S. S., A Mathematical Introduction to Robotic Manipulation, Boca Raton, FL: CRC Press, 1994, 34—61, 165—167.